

# Large Igneous Provinces and the Release of Thermogenic Volatiles from Sedimentary Basins

Henrik H. Svensen<sup>1</sup>, Morgan T. Jones<sup>1</sup>, and Tamsin A. Mather<sup>2</sup>

## ABSTRACT

Large igneous provinces (LIPs) are characterized by flood basalts and extensive magmatic plumbing systems. When sills and dykes are emplaced in sedimentary basins, the heat released can result in extensive contact metamorphism and gas generation. During the past 20 years, this process has been highlighted as potentially playing a key role in terms of proposed links between LIPs and global environmental changes. The geochemistry of the sedimentary rocks that the magma intrudes, and their potential to generate thermogenic gases such as CO<sub>2</sub> and CH<sub>4</sub> during heating, are critical controlling factors.

**KEYWORDS:** volcanic basin; sill; contact metamorphism; mineral reactions; thermogenic gas; proxies

## INTRODUCTION

Large igneous provinces (LIPs) are characterized by high magma fluxes from the deep Earth to the surface via extensive transcrustal plumbing systems that alter the thermo-mechanical structure of the crust (e.g., Black et al. 2021). In many examples of continental LIPs, the magma

---

<sup>1</sup> Department of Geosciences

Sem Sælandsvei 1

University of Oslo

0371 Oslo, Norway

E-mail: [hensven@geo.uio.no](mailto:hensven@geo.uio.no)

E-mail: [t.jones@geo.uio.no](mailto:t.jones@geo.uio.no)

<sup>2</sup> Department of Earth Sciences

University of Oxford

South Parks Road

Oxford OX1 3AN, United Kingdom

E-mail: [Tamsin.Mather@earth.ox.ac.uk](mailto:Tamsin.Mather@earth.ox.ac.uk)

passed through crystalline rocks and a cover of sedimentary basins. Such sedimentary basins invaded by basaltic sills and dykes (known as *volcanic basins*) may be deeper than 10 km, and the volume of igneous intrusions is often greater than the extrusive proportion of the LIP (FIG. 1). Sills and dykes are widespread and interact with the host rocks, leading to contact metamorphism and rapid devolatilization for some lithologies (e.g., Svensen et al. 2004, 2009; Ganino and Arndt 2009). Under these circumstances, the generated fluids are dominated by H<sub>2</sub>O and carbon-bearing species that increase the aureole pore pressure, in some cases, ultimately leading to explosive degassing to the surface via hydrothermal vent complexes or breccia pipes (FIGS. 1 and 2; Manton et al. 2022). Key examples of LIPs and volcanic basins formed over the past 350 Myr include the Karoo-Ferrar LIP (the Karoo Basin), the Central Atlantic magmatic province (basins in Brazil and the United States), the Siberian Traps (the Tunguska Basin), the North Atlantic igneous province (basins along the rifted margins of Greenland, United Kingdom, and Norway), the Parana-Etendeka LIP (basins in Southern Africa and South America), the Emeishan LIP (the Sichuan Basin), the High Arctic LIP (the Sverdrup Basin and the Barents Sea basins), and the Skagerak-centered LIP (basins across central and northern Europe, including in the Oslo Rift).

LIP flood basalt volcanism can lead to extensive CO<sub>2</sub> degassing. However, the total mass, fluxes, and δ<sup>13</sup>C signature of the carbon released from primary LIP magmas are poorly constrained, and it remains debated whether such fluxes are sufficient to account for the isotopic signals and other markers of environmental perturbation observed in the sedimentary record. These uncertainties have led researchers to propose thermogenic release from intruded sediments as an important additional source of volatiles (e.g., Svensen et al. 2004). This means that, in terms of understanding carbon cycle perturbations related to LIPs, fully constraining the igneous versus thermogenic contributions is a key goal. This is, of course, in conjunction with ongoing efforts to robustly quantify alternative non-magmatic carbon sources such as gas hydrates (e.g., Gutjahr et al. 2017).

Understanding the interactions between magma and sedimentary rocks is challenging. Outcrop samples of sills and metamorphic aureoles are important sources of information, but are often difficult to access, deeply weathered, and/or include only a small number of localities over the vast scale of a LIP (e.g., Heimdal et al. 2018). On the other hand, boreholes drilled through sills and contact aureoles may provide well-preserved samples and the spatial coverage needed to draw reliable conclusions regarding both igneous and thermogenic volatile volumes, but drilling operations are expensive and therefore limited.

Another aspect of volcanic basins is that sedimentary rocks may contaminate magmas and increase the igneous volatile load. In-situ petrological investigations of sills have emphasized the role of sediment contamination of magmas via carbonate heating and melting (e.g., Wenzel et al.

2001). Sediment melting is, in most cases, restricted to sediment xenoliths, as aureole heat transport is usually efficient and, therefore, country rock melting temperatures are not exceeded. For example, for a basaltic sill of 1100 °C emplaced at 4 km depth (100 °C ambient temperature in a normal geothermal gradient), the maximum aureole temperature close to the sill is approximately 600 °C (combined sill and background temperature divided by two). This is not high enough to initiate melting. Notable exceptions occur during prolonged magma flow in sheet intrusions, when the sill and background countryrock temperature is high, or when the sills are emplaced in rocks with low thermal conductivity, such as organic-rich shale and coal (Furlong et al. 1991; Aarnes et al. 2010).

In addition to field studies, geochemical modeling of magma–sediment interactions and experiments can yield important insights into these processes. However, such studies are limited because thermodynamic data are sparse for key intruded non-silicate materials such as carbonates, coal, organic matter, and evaporitic sulfates and halides. Direct experimental investigation of magma–sediment interaction (using a high pressure–temperature apparatus) has so far largely been restricted to studies involving magmatic assimilation of shale, but are a promising route for future insights (e.g., Deegan et al. 2022).

In this short review, we focus on the two most volumetrically important aspects of the shallow parts of LIPs: the sills and their contact aureoles. The main themes relate to how the sedimentary rock devolatilizes during heating, the carbon geochemistry of the contact aureoles, the challenges related to sedimentary proxies for LIP emplacement, and the upscaling of igneous and thermogenic gas volumes from single localities to LIP-scale.

## **PETROLOGY AND GEOCHEMISTRY OF CONTACT METAMORPHISM**

Contact metamorphism of sedimentary rocks is ongoing today in many places, and the resulting hydrothermal activity can be studied in detail. Examples include the spreading axis and basins from the Gulf of California and northwards into the USA, and in volcanic arcs such as in Indonesia. In these settings, the challenge is often that we have access to the fluids released at, or near, the surface—but seldomly those at the deep-seated intrusions or contact aureoles. These active hydrothermal systems may have started 100–1000s of years ago, and the emitted water and gas sampled at the surface represent mixed igneous, metamorphic, and sedimentary sources (e.g., Procesi et al. 2019). All of these factors make it challenging to relate the processes in modern settings to examples in the geological record that may be operating with significantly different conditions.

A key aspect for understanding how contact metamorphism may contribute to environmental changes is to investigate the behavior of key elements in contact aureoles. When studying old contact aureoles, we have to use the remaining minerals and organic matter to reconstruct what happened during progressive metamorphism, from background diagenetic conditions to high-grade metamorphism, which in some cases, may reach conditions where the rocks start to melt. For example, a typical feature of aureoles that include significant shale, especially near the contacts with intrusions >10–15 m, is the metamorphic development of a hard and compact rock texture called *hornfels*. Hornfels rocks are typically lighter in color than the rest of the aureole and contain minerals stable at high temperature and little or no remaining organic matter (FIG. 3). In the case of pelite hornfels (e.g., metamorphic shale), the minerals may include biotite, andalusite, and cordierite. Interbedded shale-carbonate lithologies develop into calc-hornfels with calc-silicate minerals (e.g., epidote, plagioclase, and clinopyroxene). We can thus use hornfels as a visual proxy for high temperatures and near-complete carbon degassing from the inner aureole. Further from the intrusion, the effects of contact metamorphism are often harder to see and the outer aureole is thus sometimes referred to as the “cryptic” part of the aureole (Barton et al. 1991). Metamorphic effects are nonetheless evident from subtler textural and mineralogical changes, including a range of geochemical differences (e.g., variations in the content and composition of organic carbon).

### ***Rock Types and Devolatilization***

The type of sedimentary host rock and the metamorphic minerals present in a contact aureole contain information regarding the volatiles generated. As examples, we present a set of generalized reactions that take place in heated sedimentary rocks with a variety of bulk compositions (TABLE 1).

Reactions (1) and (2) occur in carbonate-rich lithologies that contain quartz, where CO<sub>2</sub> and calc-silicates (tremolite and diopside) are generated during prograde metamorphism. Thus, the calc-silicates represent mineral proxies for CO<sub>2</sub> generation together with a gradually lower carbonate content towards the intrusive contact. In rocks with different bulk rock compositions, other reactions take place. In black shale, the carbonate content is often low and the total organic carbon (TOC) content is high. This leads to a contrasting mineralogical evolution compared with carbonates (i.e., pelite mineralogy) and a dominance of silicate dehydration reactions (reaction 3). As the TOC content in black shale may reach 4–5 wt.% (more than ca. 10–13 % by volume) and often above 10 wt.% TOC, the organic matter plays an important role in both gas and porosity generation. The TOC (kerogen) breaks down to thermogenic gas during metamorphism, with hydrocarbons, such as ethane and propane, formed in the low to middle temperature range (up

to 250 °C). Marine kerogen devolatilization can be described by a generalized reaction (reaction 4A), leading to a rapid increase in the pore pressure in the aureole, triggering fracturing and fluid migration (Aarnes et al. 2010). In the case of coal metamorphism (reaction 4B), the oxygen content is initially low and results in formation of reduced gases, including hydrocarbons, during devolatilization. Methane and other hydrocarbons form continuously as temperature increases (e.g., Goodarzi et al. 2018). The lowering of TOC in shale contact aureoles during progressive metamorphism is a measure of gas generation (e.g., Aarnes et al. 2010), but is not as pronounced in coal aureoles, probably due to the large size of the TOC reservoir (>50 wt.%).

Black shales are often deposited during marine anoxic and/or sulfidic conditions, resulting in high contents of metals and pyrite. Metals with an affinity for organic matter, such as Ni, Cd, V, Mo, and Hg, are potentially released from the kerogen during progressive metamorphism and follow the gas/fluid phase to the surface (see Svensen et al. 2023) or may precipitate in or around the aureole following reactions involving sulfides or organic matter. Reaction (5) describes the breakdown of sedimentary pyrite to metamorphic pyrrhotite in organic carbon-bearing shale, which liberates H<sub>2</sub>S. Reactions involving sulfur in contact metamorphic systems are complex, but likely add to the sulfur degassed from LIP magmas (Yallup et al. 2013).

Two of the LIPs associated with two of the biggest mass extinctions, the Siberian Traps and the CAMP, are characterized by abundant thick sills that were emplaced in evaporites (e.g., Svensen et al. 2009; Heimdal et al. 2018). The severity of the environmental disturbance during these LIP events may therefore be a direct result of the composition of the gases being generated in their respective volcanic basins (e.g., Svensen et al. 2009; Black et al. 2014). The affected evaporites range in composition from pure halite to pure anhydrite. Note that anhydrite is thermally stable during metamorphism, but may break down as a consequence of either dissolution in saline pore fluids or by sulfate reduction involving hydrocarbons (reaction 6). Finally, hydrocarbons in evaporites may break down to methyl groups and react with halogens to form halocarbons (CH<sub>3</sub>Cl, CH<sub>3</sub>Br; reaction 7), or react with sulfur to generate mercaptan (CH<sub>3</sub>SH), as suggested by heating experiments conducted on rocks from the Tunguska Basin (Svensen et al. 2009).

### ***Gas Speciation and Carbon Isotopes***

When seeking to understand how contact metamorphism may have affected past environments, the elements of interest include carbon, sulfur, halogens, and trace metals such as mercury. In sedimentary rocks, these elements primarily occur in organic matter, hydrocarbons, carbonates, sulfides, and sulfates. During metamorphism, the generated volatiles include reduced and

oxidized species ( $\text{CH}_4/\text{CO}/\text{CO}_2$ ,  $\text{H}_2\text{S}/\text{SO}_2$ ,  $\text{CH}_3\text{Hg}/\text{Hg}^0$ ). In addition, both nitrogen- and halogen-bearing compounds, including  $\text{CH}_3\text{Cl}$ , may form from organic matter, as mentioned above.

Carbon isotopes are a very important part of understanding potential LIP-environment links and are input parameters into carbon cycle models used for comparison with global sedimentary carbon isotope records. During progressive metamorphism, the presence of organic matter in the contact aureole will result in fluids that contain  $\text{CO}_2$  and  $\text{CH}_4$  (e.g., such as reactions (1) and (2) in TABLE 1), which will affect carbon isotopic signatures. The isotopic composition of the generated carbon gas at a given temperature depends both on the carbon source (carbonate versus TOC, and the amount and type of TOC) and speciation (i.e., isotope fractionation differs between  $\text{CH}_4$  and  $\text{CO}_2$ ). Carbon dioxide generated from carbonates will inherit the isotopic signature of the host sediment, modified by a temperature-dependent fractionation. The result is thermogenic  $\text{CO}_2$  with a  $\delta^{13}\text{C}$  value usually between  $-8\text{‰}$  and  $-2\text{‰}$ . If the main organic source is marine algae, the gas will be dominated by  $\text{CH}_4$  with a  $\delta^{13}\text{C}$  signature typically between  $-33\text{‰}$  to  $-26\text{‰}$ , slightly  $^{12}\text{C}$ -enriched compared with the bulk rock TOC. Nonetheless, the thermogenic gas will still contain some  $\text{CO}_2$  and potentially other hydrocarbons (e.g., ethane, propane). As the temperature in the aureole rises further, the generated gas will be increasingly enriched in dry gas ( $\text{CH}_4$  and  $\text{CO}_2$ ) instead of the higher hydrocarbons.

Experimental and theoretical studies have shown that a large isotopic fractionation occurs between  $\text{CH}_4$  and  $\text{CO}_2$ , decreasing with increasing temperature (see Kueter et al. 2019). Below  $300\text{ °C}$ , corresponding to temperatures characteristic of the outer regions of contact aureoles, the  $^{12}\text{C}$  is enriched in  $\text{CH}_4$  by  $25\text{‰}$ – $35\text{‰}$  compared with  $\text{CO}_2$ . At higher temperatures, the  $^{12}\text{C}/^{13}\text{C}$   $\text{CO}_2$ - $\text{CH}_4$  fractionation is less (around  $12\text{‰}$  at  $600\text{ °C}$ ). Together with the varying source composition of the TOC, this fractionation explains the typical coexisting low  $\delta^{13}\text{C}$  ( $\text{CH}_4$ ) and high  $\delta^{13}\text{C}$  ( $\text{CO}_2$ ) values of thermogenic gas. When studying contact aureoles, the gas is usually long gone and we have to focus on the remaining organic matter or graphite. Data reported from numerous case studies have shown that the aureole TOC in marine sediments has  $\delta^{13}\text{C}$  values within  $2\text{‰}$  of the values in the background unaltered sediment. Contact aureoles in coal show more complex  $\delta^{13}\text{C}_{\text{TOC}}$  behavior compared with those in shales. The span in  $\delta^{13}\text{C}_{\text{TOC}}$  in case studies from metamorphic coal ranges from  $-22\text{‰}$  to  $-26\text{‰}$  largely due to the presence of different types of organic matter (macerals), as shown by organic petrography (e.g., liptinite/vitrinite/inertinite) (e.g., Sanders et al. 2023). This suggests that in contact aureoles, isotopically light gas ( $\text{CH}_4$  and higher hydrocarbons) is balanced by isotopically heavy gas ( $\text{CO}_2$  and  $\text{CO}$ ), which conserves the pre-metamorphic bulk rock  $\delta^{13}\text{C}_{\text{TOC}}$  within a few per mil. Thus, the contact aureole  $\delta^{13}\text{C}_{\text{TOC}}$  is likely not a proxy for thermogenic gas generation.

Overall, this means that we have to consider both the geochemical and petrological archive remaining in the aureole long after metamorphism has ceased, as well as theoretical and experimental studies on the evolution of gas speciation and isotope fractionation, from diagenetic to peak metamorphic conditions.

### ***Aureole Parameters and Aureole Proxies***

The typical parameters studied in contact aureoles are related to: 1) geochemical variation of elements towards the intrusions (TOC,  $\delta^{13}\text{C}$  of carbonates and TOC, element concentrations, organic pyrolysis); 2) temperature proxies (e.g., vitrinite reflectance and mineralogy); and 3) physical properties reflecting changes in mineralogy and textures (e.g., seismic velocities, density). In thermal models, theoretical TOC predictions are compared to measured TOC to tune the model outputs, and the predicted TOC loss is then converted to a mass of  $\text{CO}_2$  (e.g., Iyer et al. 2018). Carbon dioxide generation from reactions involving carbonates may also be included in such models, but gas speciation is not. This means that the  $\text{CO}_2$  to  $\text{CH}_4$  ratio is poorly constrained both from a model and proxy perspective, and depends both on the initial kerogen composition and the oxygen fugacity during contact metamorphism. The gas generation in aureole models is a function of temperature, and the modeled aureole temperature is tuned to the calculated and measured vitrinite reflectivity. Moreover, although such models are made for sill–aureole systems, thermal models do not include fluid transport processes (e.g., Galerne and Hasenclever 2019). Data constraints on fluid flow models pose further challenges, as they require a comprehensive dataset of temperature proxies. Finally, the fate of the gases or fluids generated in contact aureoles is crucial for understanding the possible environmental consequences, as addressed later in this review. Other processes can alter thermogenic release rates even after volatile emission from the crust. For example, for submarine degassing, dissolution of soluble gases into aqueous solution may influence how much of the thermogenic gases eventually reach the atmosphere.

## **THE PROXY CHALLENGE**

A critical issue with assessing the importance of LIP activity as a driver of environmental change is how to trace the effects of the release of volcanic and thermogenic gas to the ocean–atmosphere system. So far, no specific sedimentary proxies are available for thermogenic gas release and/or the formation of hydrothermal vent complexes in sedimentary basins. Several proxies are used for extrusive LIP activity. Tephra layers represent a near-field proxy and Os isotopes have been widely used to infer LIP-related weathering or LIP-associated hydrothermal activity (Percival et

al. 2018 and references therein). Sedimentary Hg contents and isotopes have been used as a volcanic proxy in numerous studies during the past decade (e.g., Grasby et al. 2019 and references therein). Mercury has the advantage that volcanic emissions represent a major flux into the environment, and, thus, it can be used as a direct proxy of volcanic gas emission to the atmosphere. Moreover, its long atmospheric lifetime (6–18 months) offers the potential to detect global distributions (Pyle and Mather 2003). Prolonged periods of elevated volcanic activity, such as those that produced LIPs, can directly impact the Hg cycle, resulting in Hg enrichments in catchments well away from the source volcanism (Grasby et al. 2019). In the case of submarine degassing, Hg is rapidly scrubbed into the water column, restricting subsequent deposition to localities proximal to the source.

As a widespread marker potentially tracing igneous degassing processes, understanding the Hg proxy in terms of thermogenic LIP fluxes has particular relevance. The main depositional pathway for Hg into sediments in aqueous environments is associated with organic matter. Therefore, peaks in Hg/TOC (total organic carbon) ratios are often interpreted to reflect increases in Hg to the catchment, either through the enrichment of Hg in organic matter or via deposition through other pathways such as sulfides (Sanei et al. 2012). Importantly, the strong affinity to organic matter leads to Hg enrichments in organic-rich sediments, and the devolatilization of these TOC-rich strata during contact metamorphism may also liberate significant quantities of Hg that may make it to the atmosphere (Svensen et al. 2023). Therefore, far-field Hg enrichments cannot currently differentiate between volcanic and thermogenic Hg sources, unless there is a clear distinction in subaerial versus submarine degassing between volcanic and thermogenic sources in the LIP (e.g., Jones et al. 2019a).

Several studies have begun utilizing Hg isotopes to further develop this element's potential as a volcanic proxy. Mercury is highly volatile and susceptible to changes in redox conditions, leading to several fractionation processes (e.g., Bergquist and Blum 2007). In particular, mass independent fractionation (MIF; e.g.,  $\Delta^{199}\text{Hg}$ ) signatures, have been cited as evidence for direct atmospheric deposition from several LIPs such as the Central Atlantic magmatic province (CAMP; Shen et al. 2022). However, this field of study is in its infancy, as there are several contemporaneous processes that might affect MIF values. It is thus unclear how contact metamorphism may affect the isotopic signature of Hg emissions volatilized and transported to the surface. In summary, there are currently no rigorous approaches that reliably discern between volcanic and thermogenic activity in the far-field proxy record.

## **THERMOGENIC EMISSIONS AND ENVIRONMENTAL CONSEQUENCES**



LIPs and volcanic basins are a setting where elements may get mobilized and emitted to the atmosphere on very short geological timescales. Since the 1970s, degassing of CO<sub>2</sub> and SO<sub>2</sub> from LIP lavas has been regarded as a key process in modifying the climate and environment. Lava degassing is easy to visualize because it happens today and can be observed and studied, albeit on a much smaller scale than for LIPs. Contact metamorphic degassing is, on the other hand, much less studied and often associated with uncertainties regarding the volumes and fate of the gas. It is therefore interesting to compare thermogenic and igneous CO<sub>2</sub> estimates. The volcanic gas emissions from LIPs are often based on poorly constrained lava volumes, assumptions about the CO<sub>2</sub> mass per km<sup>3</sup>, and CO<sub>2</sub> isotopic compositions based on mid-ocean ridge lavas. Due to the strong pressure dependence of CO<sub>2</sub> solubility in basaltic melt, it can start to exsolve at depths of 30–40 km. A common assumption is that CO<sub>2</sub> migrates together with the ascent of magma, potentially with an early and deep-seated CO<sub>2</sub> pulse prior to the main lava stage (e.g., Nava et al. 2021). In such a scenario the atmospheric CO<sub>2</sub>-release is not directly proportional to the erupted lava volume, and CO<sub>2</sub> may seep through country rocks or follow the magmatic plumbing system and interact with magma at shallower levels. The pathways and processes involved when igneous CO<sub>2</sub> is degassed from magma clearly deserve further attention and case studies. Keeping this in mind, we turn to the thermogenic estimates.

As presented earlier, many reactions contribute to metamorphic devolatilization (TABLE 1), and aureole geochemistry contains information that can be used to quantify the carbon, sulfur, and metals lost during metamorphism. We can use such measurements to upscale data from a single locality or borehole (i.e., a 1-m<sup>2</sup> column through the aureole) to the full volume of the sill–aureole system and, further, to the scale of the studied region or volcanic basin. Depending on the assumptions used, such upscaling is usually limited to yielding an upper limit of thermogenic gas generated and potentially released to the ocean or atmosphere. This method requires the contact aureole volume (area  $A$  × thickness  $h$ ) and the amount of TOC (or other volatile) missing from the aureole in wt.%,  $F_c$  (i.e., the lowering of the aureole TOC). The total mass of carbon,  $W_c$ , produced in contact aureoles is:  $W_c = F_c \times A \times h \times \rho$ , where  $\rho$  is the rock density (kg/m<sup>3</sup>). The area  $A$  is measured from seismic or field data. As a rule of thumb (there are notable exceptions, as mentioned earlier), the aureole has a width that equals the sill thickness on each side of the sill, i.e., double the sill volume. The thickness  $h$  of the contact aureole can thus be approximated from the sill volume or from field data associated with the contact aureole, such as TOC and vitrinite reflectivity data. The total mass of carbon produced,  $W_c$ , can be converted to equivalents of methane (=  $W_c \times 1.34$ ) and/or carbon dioxide (=  $W_c \times 3.66$ ). This approach is simple with many assumptions and uncertainties, in particular regarding lateral heterogeneities and contact aureole volumes, but may be supplemented and further constrained by statistical methods (e.g.,

Jones et al. 2019b) and models that account for the heat transport by fluid flow in cases where the host rocks have high porosities (e.g., Galerne and Hasenclever 2019).

A key question is what happens to thermogenic gases following their migration out of the contact aureoles. Realistic scenarios include explosive release during hydrofracturing and venting, slower seepage and release at the surface (cf. the deep igneous degassing scenario mentioned above), or permanent storage at shallower basin levels. Numerous studies have shown that hydrothermal vent complexes (also known as breccia pipes) are common in volcanic basins. They provide direct evidence for rapid gas release to the atmosphere, often followed by prolonged seepage activity through the conduit (e.g., Svensen et al. 2004; Manton et al. 2022). Modeling studies have suggested that fracture generation and permeability (i.e., vent initiation) are at least three times more efficient in transferring gas to the surface than a scenario without venting such as seepage (Galerie and Hasenclever 2019). The scenario of permanent storage of thermogenic gas in reservoirs is, in cases such as the Karoo Basin and others, not considered significant due to the absence of major thermogenic gas accumulations. Furthermore, available seismic interpretations from volcanic basins show well-developed permeability pathways associated with sills and vents, supporting the hypothesis that thermogenic gas eventually migrated to the surface (Manton et al. 2022).

FIGURE 4 shows a summary of our review of degassing from LIPs. When combining estimates of contact aureole gas speciation, isotopic composition and volume, the results can be used in Earth system models to assess causal relationships between the LIP degassing augmented by thermogenic release, and atmospheric and climatic changes. Further constraints from high-precision dating of sills are needed in combination with statistical approaches to understanding sill emplacement and degassing (Jones et al. 2019b). In this way, the understanding of LIPs and the geological processes taking place during magma emplacement represents an increasingly robust background to studies of rapid global changes over timescales of centuries to millennia.

## **CONCLUSIONS**

We summarize our review in four bullet points:

- Volcanic basins are a key setting that can shed new light on how LIPs have affected the environment via studies of magma–sediment interactions.
- Different sedimentary rock types are affected by the heat from sills and dykes in varying ways, but a series of fundamental reactions can be used to systematize these processes.

For example, we use both organic and inorganic petrology and geochemistry to reconstruct the devolatilization history of contact aureoles.

- Current proxies in the sedimentary record for LIP gas release, such as mercury, cannot reliably distinguish between igneous and thermogenic sources, and there is a need to refine and develop new proxies.
- Upscaling estimates of thermogenic emission fluxes from sparse measurements and making comparisons to igneous degassing is important, but these improvements require more extensive field data and developments in our process understanding.

## ACKNOWLEDGMENTS

We acknowledge support from the Norwegian Research Council (grant 263000 to M.T.J., and grant 223272 to H.H.S. and M.T.J. as part of the Centre for Earth Evolution and Dynamics). T.A.M. acknowledges funding from ERC consolidator grant (ERC-2018-COG-818717-V-ECHO). We thank Victoria Hovland and Caroline S. Hovland for making Figure 4A. Finally, we thank three anonymous referees for constructive comments, and Sverre Planke and Alexander Polozov for discussions and lasting enthusiasm.

## REFERENCES

- Aarnes I, Svensen H, Connolly JAD, Podladchikov YY (2010) How contact metamorphism can trigger global climate changes: modeling gas generation around igneous sills in sedimentary basins. *Geochimica Et Cosmochimica Acta* 74: 7179-7195, doi: [10.1016/j.gca.2010.09.011](https://doi.org/10.1016/j.gca.2010.09.011)
- Barton MD, Staude J-M, Snow EA, Johnson DA (1991) Aureole systematics. In: Kerrick DM (ed) *Contact Metamorphism, Reviews in Mineralogy and Geochemistry, Volume 26*. Mineralogical Society of America, Chantilly, pp 723-847, doi: [10.1515/9781501509612-017](https://doi.org/10.1515/9781501509612-017)
- Bergquist BA, Blum JD (2007) Mass-dependent and -independent fractionation of Hg isotopes by photoreduction in aquatic systems. *Science* 318: 417-420, doi: [10.1126/science.1148050](https://doi.org/10.1126/science.1148050)
- Black BA, Lamarque JF, Shields CA, Elkins-Tanton LT, Kiehl JT (2014) Acid rain and ozone depletion from pulsed Siberian Traps magmatism. *Geology* 42: 67-70, doi: [10.1130/G34875.1](https://doi.org/10.1130/G34875.1)
- Black BA, Karlstrom L, Mather TA (2021) The life cycle of large igneous provinces. *Nature Reviews Earth & Environment* 2: 840-857, doi: [10.1038/s43017-021-00221-4](https://doi.org/10.1038/s43017-021-00221-4)
- Deegan FM and 12 coauthors (2022) Magma–shale interaction in large igneous provinces: implications for climate warming and sulfide genesis. *Journal of Petrology* 63: egac094, doi: [10.1093/petrology/egac094](https://doi.org/10.1093/petrology/egac094)

- Furlong KP, Hanson RB, Bowers JR (1991) Modeling thermal regimes. In: Kerrick DM (ed) Contact Metamorphism, Reviews in Mineralogy and Geochemistry, Volume 26. Mineralogical Society of America, Chantilly, pp 437-505, doi: [10.1515/9781501509612-013](https://doi.org/10.1515/9781501509612-013)
- Galerne CY, Hasenclever J (2019) Distinct degassing pulses during magma invasion in the stratified Karoo Basin—new insights from hydrothermal fluid flow modeling. *Geochemistry, Geophysics, Geosystems* 20: 2955-2984, doi: [10.1029/2018GC008120](https://doi.org/10.1029/2018GC008120)
- Ganino C, Arndt NT (2009) Climate changes caused by degassing of sediments during the emplacement of large igneous provinces. *Geology* 37: 323-326, doi: [10.1130/G25325A.1](https://doi.org/10.1130/G25325A.1)
- Goodarzi F, Gentzis T, Grasby SE, Dewing K (2018) Influence of igneous intrusions on thermal maturity and optical texture: comparison between a bituminous marl and a coal seam of the same maturity. *International Journal of Coal Geology* 198: 183-197, [10.1016/j.coal.2018.09.013](https://doi.org/10.1016/j.coal.2018.09.013)
- Grasby SE, Them II TR, Chen Z, Yin R, Ardakani OH (2019) Mercury as a proxy for volcanic emissions in the geologic record. *Earth-Science Reviews* 196: 102880, doi: [10.1016/j.earscirev.2019.102880](https://doi.org/10.1016/j.earscirev.2019.102880)
- Gutjahr M and 8 coauthors (2017) Very large release of mostly volcanic carbon during the Palaeocene–Eocene Thermal Maximum. *Nature* 548: 573-577, doi: [10.1038/nature23646](https://doi.org/10.1038/nature23646)
- Heimdal TH and 7 coauthors (2018) Large-scale sill emplacement in Brazil as a trigger for the end-Triassic crisis. *Scientific Reports* 8: 141, doi: [10.1038/s41598-017-18629-8](https://doi.org/10.1038/s41598-017-18629-8)
- Iyer K, Svensen H, Schmid DW (2018) SILLi 1.0: a 1D numerical tool quantifying the thermal effects of sill intrusions. *Geoscientific Model Development* 11: 43–60, doi: [10.5194/gmd-11-43-2018](https://doi.org/10.5194/gmd-11-43-2018)
- Jones MT and 10 coauthors (2019a) Mercury anomalies across the Palaeocene–Eocene Thermal Maximum. *Climate of the Past* 15: 217-236, doi: [10.5194/cp-15-217-2019](https://doi.org/10.5194/cp-15-217-2019)
- Jones SM, Hoggett M, Greene SE, Dunkley Jones T (2019b) Large igneous province thermogenic greenhouse gas flux could have initiated Paleocene–Eocene Thermal Maximum climate change. *Nature Communications* 10: 5547, doi: [10.1038/s41467-019-12957-1](https://doi.org/10.1038/s41467-019-12957-1)
- Kueter N, Schmidt MW, Lilley MD, Bernasconi SM (2019) Experimental determination of equilibrium CH<sub>4</sub>–CO<sub>2</sub>–CO carbon isotope fractionation factors (300–1200 °C). *Earth and Planetary Science Letters* 506: 64-75, doi: [10.1016/j.epsl.2018.10.021](https://doi.org/10.1016/j.epsl.2018.10.021)
- Manton B and 9 coauthors (2022) Characterizing ancient and modern hydrothermal venting systems. *Marine Geology* 447: 106781, doi: [10.1016/j.margeo.2022.106781](https://doi.org/10.1016/j.margeo.2022.106781)
- Nava A and 5 coauthors (2021) Reconciling early Deccan Traps CO<sub>2</sub> outgassing and pre-KPB global climate. *Proceedings of the National Academy of Sciences* 118: e2007797118, doi: [10.1073/pnas.2007797118](https://doi.org/10.1073/pnas.2007797118)
- Percival LME, Jenkyns HC, Mather TA, Dickson AJ, Batenburg SJ, Ruhl M, Hesselbo SP, Barclay R, Jarvis I, Robinson SA, Woelders L (2018) Does large igneous province volcanism always perturb the mercury cycle? Comparing the records of Oceanic Anoxic Event 2 and the end-cretaceous to other Mesozoic events. *American Journal of Science* 318: 799-860, doi.org/10.2475/08.2018.01
- Procesi M, Ciotoli G, Mazzini A, Etiope G (2019) Sediment-hosted geothermal systems: review and first global mapping. *Earth-Science Reviews* 192: 529-544, doi: [10.1016/j.earscirev.2019.03.020](https://doi.org/10.1016/j.earscirev.2019.03.020)

- Pyle DM, Mather TA (2003) The importance of volcanic emissions for the global atmospheric mercury cycle. *Atmospheric Environment* 37: 5115-5124, doi: [10.1016/j.atmosenv.2003.07.011](https://doi.org/10.1016/j.atmosenv.2003.07.011)
- Sanders MM, Rimmer SM, Rowe HD (2023) Carbon isotopic composition and organic petrography of thermally metamorphosed Antarctic coal: implications for evaluation of  $\delta^{13}\text{C}_{\text{org}}$  excursions in paleo-atmospheric reconstruction. *International Journal of Coal Geology* 267: 104182, doi: [10.1016/j.coal.2022.104182](https://doi.org/10.1016/j.coal.2022.104182)
- Sanei H, Grasby S, Beauchamp B (2012) Latest Permian mercury anomalies. *Geology* 40: 63-66, doi: [10.1130/G32596.1](https://doi.org/10.1130/G32596.1)
- Shen J, Yin R, Algeo TJ, Svensen HH, Schoepfer SD (2022) Mercury evidence for combustion of organic-rich sediments during the end-Triassic crisis. *Nature Communications* 13: 1307, doi: [10.1038/s41467-022-28891-8](https://doi.org/10.1038/s41467-022-28891-8)
- Svensen H and 6 coauthors (2004) Release of methane from a volcanic basin as a mechanism for initial Eocene global warming. *Nature* 429: 542-545, doi: [10.1038/nature02566](https://doi.org/10.1038/nature02566)
- Svensen H and 6 coauthors (2009) Siberian gas venting and the end-Permian environmental crisis. *Earth and Planetary Science Letters* 277: 490-500, doi: [10.1016/j.epsl.2008.11.015](https://doi.org/10.1016/j.epsl.2008.11.015)
- Svensen HH, Jones MT, Percival LME, Grasby SE, Mather TA (2023) Release of mercury during contact metamorphism of shale: Implications for understanding the impacts of large igneous province volcanism. *Earth and Planetary Science Letters* 619: 118306, doi: [10.1016/j.epsl.2023.118306](https://doi.org/10.1016/j.epsl.2023.118306)
- Yallup C, Edmonds M, Turchyn AV (2013) Sulfur degassing due to contact metamorphism during flood basalt eruptions. *Geochimica et Cosmochimica Acta* 120: 263-279, doi: [10.1016/j.gca.2013.06.025](https://doi.org/10.1016/j.gca.2013.06.025)
- Wenzel T and 5 coauthors (2001) Contamination of mafic magma by partial melting of dolomitic xenoliths. *Terra Nova* 13: 197-202, doi: [10.1046/j.1365-3121.2001.00340.x](https://doi.org/10.1046/j.1365-3121.2001.00340.x)

**TABLE 1. GENERALIZED OVERALL MINERAL REACTIONS IN CONTACT AUREOLES. NAMES ARE USED FOR ALL MINERALS AND THE REACTIONS ARE NOT BALANCED.**

- (1) Dolomite + Quartz + H<sub>2</sub>O → Tremolite + Calcite + CO<sub>2</sub>
- (2) Tremolite + Calcite + Quartz → Diopside + CO<sub>2</sub> + H<sub>2</sub>O
- (3) Smectite → Illite + H<sub>2</sub>O → Mica + Andalusite + H<sub>2</sub>O
- (4A) Marine kerogen → CH<sub>4</sub> + CO<sub>2</sub> + HC (hydrocarbons) + residual carbon
- (4B) Coal → CH<sub>4</sub> + CO + HC + residual carbon
- (5) Pyrite + H<sub>2</sub>O + C → Pyrrhotite + CO<sub>2</sub> + 2H<sub>2</sub>S
- (6) Anhydrite + CH<sub>4</sub> → Calcite + H<sub>2</sub>S + H<sub>2</sub>O
- (7) CH<sub>4</sub> + Cl<sup>-</sup> → CH<sub>3</sub>Cl + H<sup>+</sup>

SOURCES: GOODARZI ET AL. (2018), TISSOT ET AL. (1987), TRACY AND FROST (1991), SVENSEN ET AL. (2009). References are listed in the supplemental material.

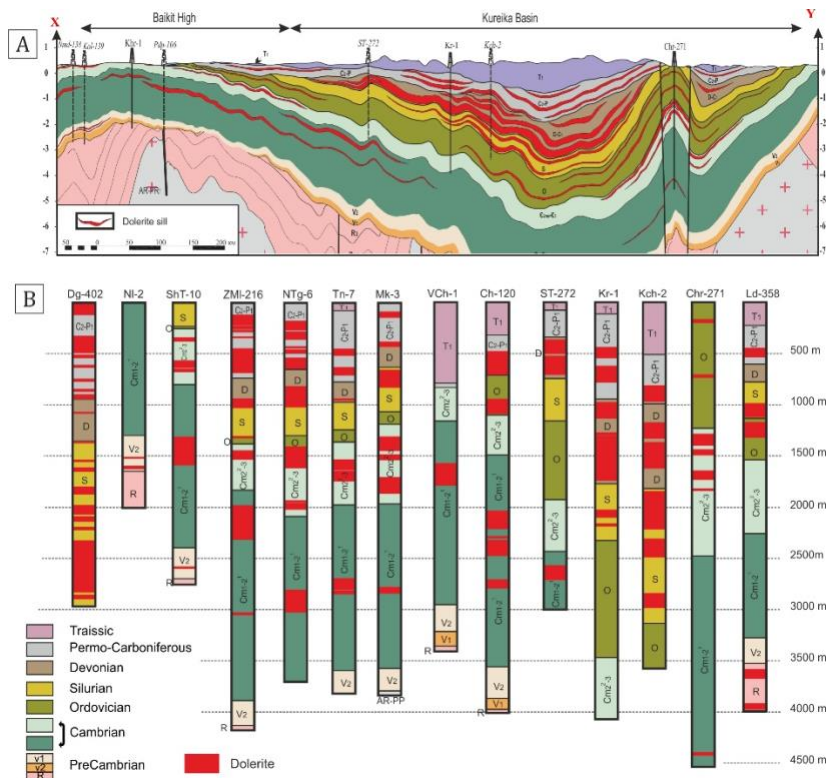


**FIGURE 1:** (A) Cross section across the Siberian Traps, from the southwest (X) to the northeast (Y). This shows extensive sills emplaced in carbonates and evaporites. Breccia pipes are numerous in the basin, originating from magma–sediment interactions, but are not shown. In addition, a variety of extrusive volcanic rocks are present, including tephtras, pyroclastic deposits, and lava flows. (B) Lithological logs from boreholes in the Tunguska Basin (Siberian Traps) showing thick dolerite sills emplaced in Cambrian and Ordovician carbonates and evaporites as part of the LIP plumbing system. MODIFIED FROM SVENSEN ET AL. (2018). References are listed in the supplemental material.



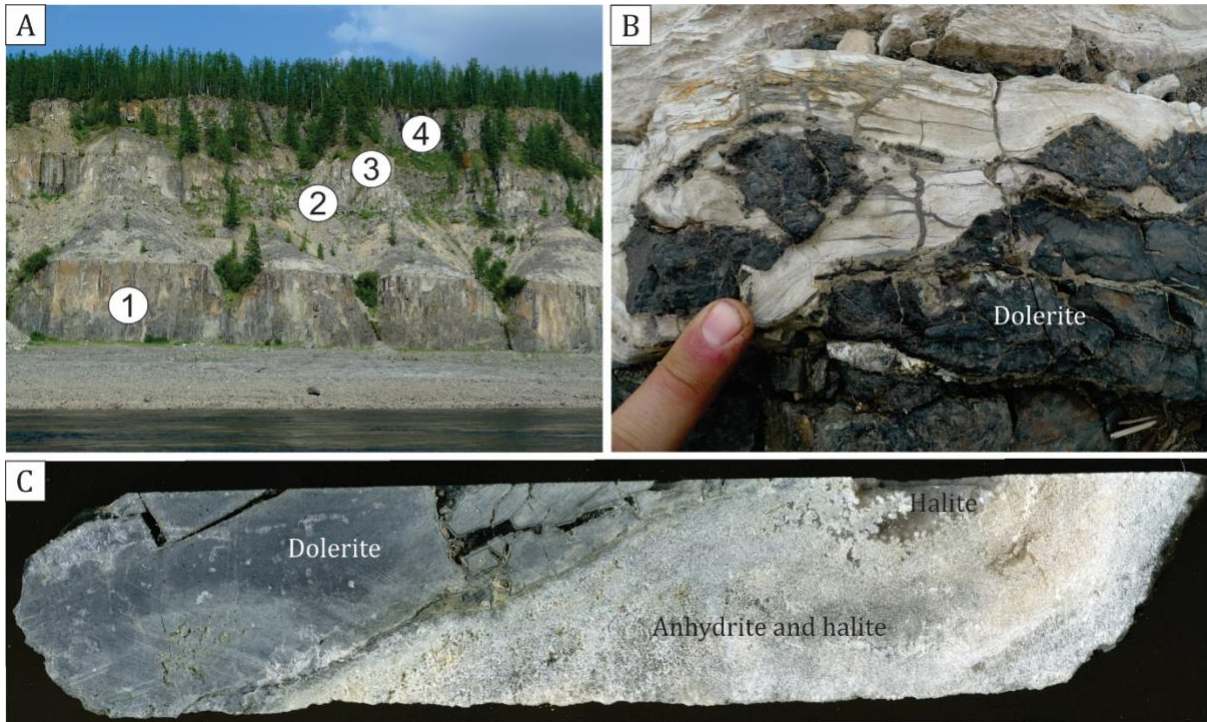


**FIGURE 2.** Examples of contact metamorphism from the Siberian Traps. **(A)** Four sills (1–4) emplaced in sandstone and coal (grey layers). **(B)** Dolerite dyke (black) emplaced in dolostone, showing dyke fragmentation and veining in the contact aureole. **(C)** Scan of a split drill core from 3001m depth in the Tunguska Basin, showing the contact between a thick dolerite dyke and evaporite with anhydrite and halite. The core sample is 20 cm long.



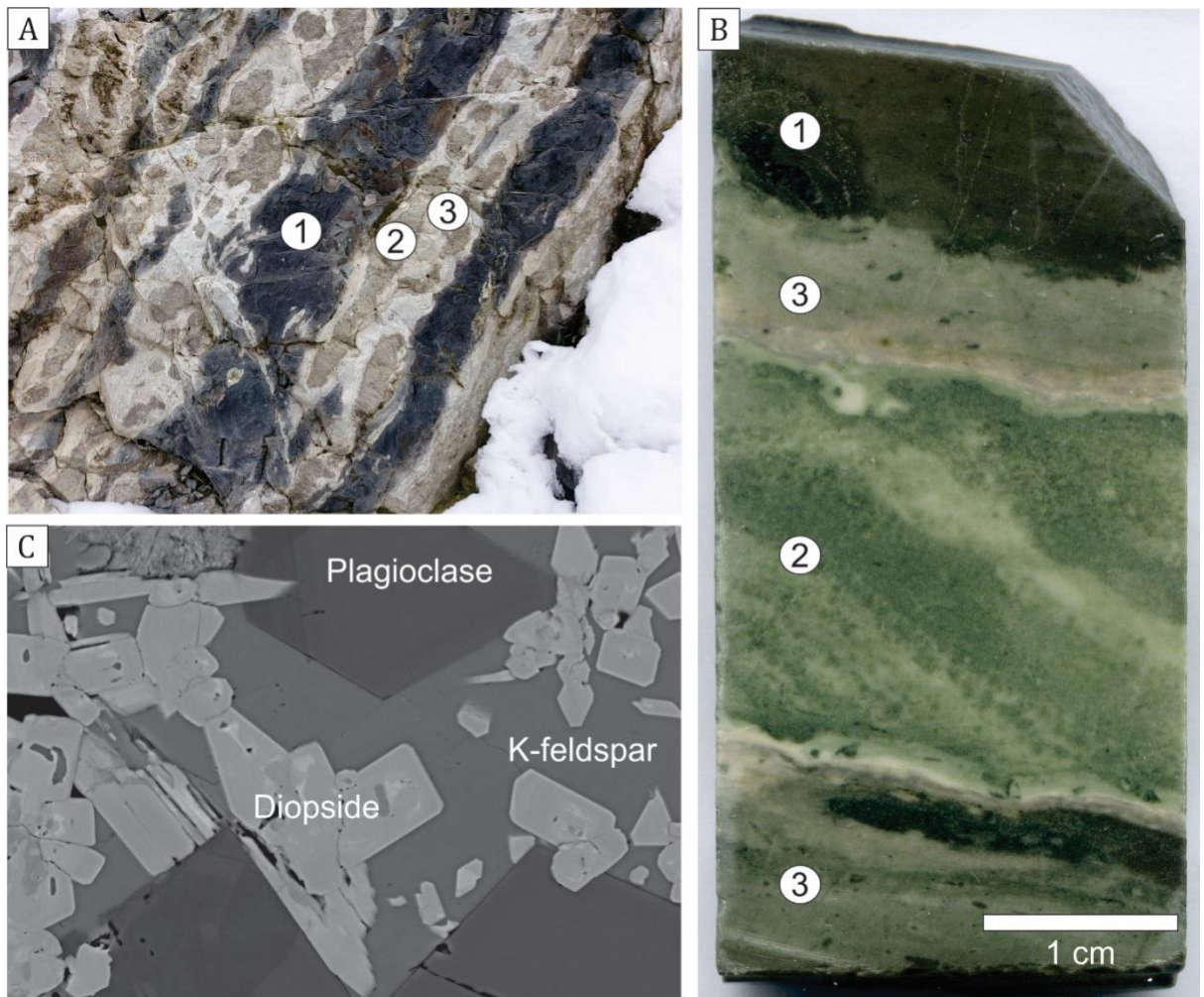


**FIGURE 3.** Hornfels from the Oslo Rift became famous following the pioneering work of Victor M. Goldschmidt more than a century ago. **(A)** shows a typical hornfels outcrop near Oslo, where the dark layers (1) represent former Ordovician shale and the light green layers (2) are former limestone nodules. During contact metamorphism, these two rock types became hornfels—with a reaction zone (3) developed due to a diffusion-controlled gradient in the carbonate content. The width of zone 1 and 2 is ca. 20cm. **(B)** Cut and scanned sample across a former limestone nodule (2) in shale (1), where the reaction zone (3) with shale is well developed. The devolatilization reactions resulted in formation of  $\text{CO}_2$  and calc-silicates, such as green diopside and plagioclase, as shown in the back-scattered electron image from zone (2). Note the absence of carbonate, which indicates that the reactions consumed all of the original calcite. Photos by H.H. Svensen.

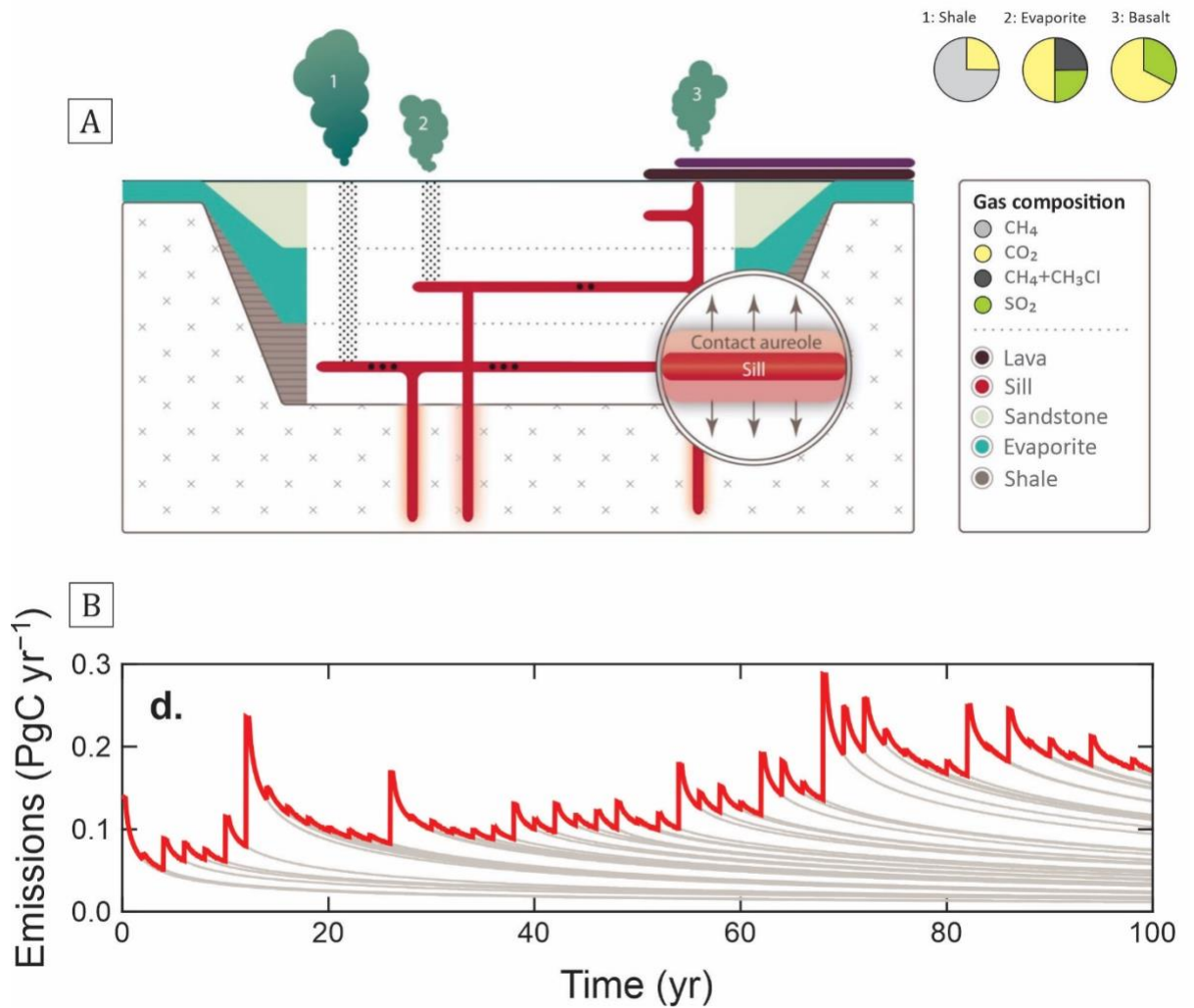


**FIGURE 4.** (A) Generalized LIP cross section through a volcanic basin. The figure is based on seismic interpretations and field mapping in volcanic basins. Schematic gas compositions from metamorphism of shale (1) and evaporite (2), and flood basalt degassing (3). (B) Modeled flux of thermogenic CH<sub>4</sub> based on theoretical and pulsed sill emplacement in the North East Atlantic Igneous Province (56 Ma; Jones et al. 2019b). Together with values for the  $\delta^{13}\text{C}$  of the methane released, these data are used in carbon cycle models to calculate the effects on the surface carbon reservoir and compared to sedimentary carbon isotope records.